Int J Thermophys
DOI 10.1007/s10765-009-0555-9

# Study of Au, Ni-(n)ZnSe Thin Film Schottky Barrier Junctions

**Sumbit Chaliha · Mothura Nath Borah · P. C. Sarmah · A. Rahman**



**Abstract** Schottky barrier junctions of Al-doped n-type Zinc selenide (ZnSe) thin films of doping concentrations up to $9.7 \times 10^{14} \mathrm{cm}^{-3}$ have been fabricated with Au and Ni electrodes on glass substrates by sequential thermal evaporation. All of the junctions of different doping concentrations exhibited rectifying current-voltage characteristics with a non-saturating reverse current. From the current-voltage characteristics, the different junction parameters such as ideality factor, saturation current density, series resistance, etc., were measured. Both types of junctions were found to possess a high ideality factor and a high series resistance. The barrier heights of the junctions were measured from Richardson plots and found to be around 0.8 eV. The structures were found to exhibit a poor photovoltaic effect with a fill factor not greater than 0.4. The diode quality as well as the photovoltaic performance of the diodes were improved following a short heat treatment in vacuum.

**Keywords** Diode ideality factor · Schottky barrier · Thermal evaporation · Zinc selenide

S. Chaliha (✉)
Department of Physics, Bahona College,
Jorhat 785101, India
e-mail: sumbitc@gmail.com

M. N. Borah
Department of Physics, D. R. College, Golaghat 785621, India

P. C. Sarmah
Electronics Division, North East Institute of Science and Technology,
Jorhat 785006, India

A. Rahman
Department of Physics, Gauhati University,
Guwahati 781014, India

Published online: 23 January 2009

## 1 Introduction

Zinc selenide (ZnSe), a II–VI compound semiconductor with a 2.67 eV direct bandgap, has long been considered to be a promising material for different optoelectronic devices such as LEDs, thin film transistors, blue laser diodes, photodetectors, and thin-film solar cells [1–4]. There are a number of reports on the structural, optical, and electrical properties of ZnSe polycrystalline thin films prepared by various techniques such as chemical vapor deposition, chemical deposition, and physical vapor deposition [5–8]. Although many investigations on the formation of Schottky barriers with single crystal bulk ZnSe using different metals have been carried out [3,9,10], little attention has been given to Schottky barriers formed with polycrystalline ZnSe thin films. Thin-film Schottky barriers are attractive for photodetectors and thin-film solar cells due to their easy fabrication. Thermal evaporation is also cost effective and suitable for large area deposition. In the present work, (n)ZnSe thin-film Schottky barrier junctions with Au and Ni barrier metals have been prepared by thermal evaporation. Since the annealing process plays an important role in enhancing the performance of thin-film devices [11], the prepared devices were also subjected to a short heat treatment. Studies of various junction parameters and photovoltaic performance of these Schottky barrier junctions, measured before and after heat treatment, are reported in this article.

## 2 Experimental

The samples were prepared on glass substrates by sequential thermal evaporation at a base pressure of $5 \times 10^{-5}$ Torr. First, the ohmic contacts formed from five parallel strips of aluminum, each of 1 mm width and 20 mm length, were thermally deposited over glass slides using an electrically heated tungsten spiral. Above these strips, Al-doped ZnSe films of $15 \times 15\,\text{mm}^2$ area were thermally deposited by co-evaporation of ZnSe powder (99.99 %) from an electrically heated molybdenum boat and Al metal (99.9 %) from the tungsten spiral filament. The Al doping makes ZnSe an n-type semiconductor. At the time of deposition, the substrate temperature was maintained at 473 K. Three sets of Al-doped ZnSe films of different doping concentrations were prepared by maintaining a constant deposition rate for ZnSe and changing the evaporation rate of Al. After deposition, the films were annealed in vacuum at 523 K for 60 min. Finally, for the barrier metal, five Au and five Ni electrodes (each of 1 mm width) were vacuum deposited separately over the three sets of Al-doped ZnSe films using suitable masks. Thus, three sets of Al-(n)ZnSe-Au structures and three sets of Al-(n)ZnSe-Ni structures of different doping concentrations with 25 junctions of $1\,\text{mm}^2$ area each have been prepared. A schematic diagram of the structure of the devices having 25 and 9 Au-(n)ZnSe Schottky barrier junctions is shown in Fig. 1.

For measurement of the conductivity type, thickness, and other properties, separate films were deposited at the time of respective semiconducting film deposition by placing additional substrates in the deposition system. Al electrodes were vacuum deposited on ZnSe films for conductivity measurements. The thicknesses of the films were measured by a multiple interference technique [12] and found to be around 3,000 Å to 3,500 Å. The conductivity type and carrier concentration of the films were deter-

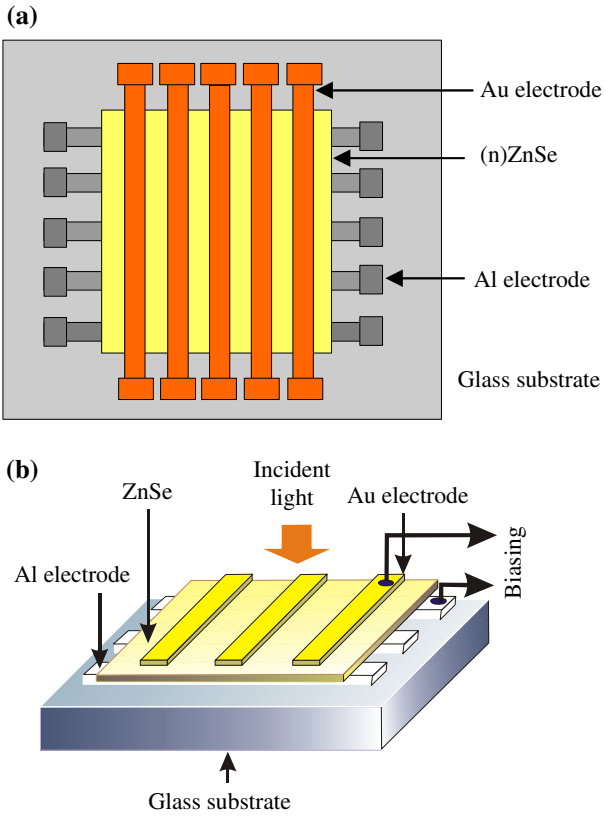


**Fig. 1** Schematic diagrams of Au-(n)ZnSe Schottky barrier: (**a**) top view and (**b**) lateral view (not to scale)

mined by Hall-effect measurements of the films and analysis of the capacitance-voltage characteristics [13] of the Schottky barriers. For films of lower doping concentrations, the hot-probe method [14] was also used to confirm the conductivity type of the film.

To avoid humidity effects, all electrical and photovoltaic measurements were made in a vacuum of $10^{-2}$ Torr by mounting the sample inside a specially assembled vacuum chamber. The details of this experimental arrangement have been discussed elsewhere [15]. A Keithley system electrometer (Model 6514) was used to measure the current in dark and under illumination. The current ($I$)-voltage ($V$) characteristics of the junctions were recorded at room temperature as well as at elevated temperatures using a temperature-controlled heating arrangement in the vacuum chamber. For studying the current-voltage characteristics under illumination, the samples in the chamber were illuminated through a glass window using a white light from a tungsten-halogen lamp. The performance of the devices was also measured after a short heat treatment (annealing) at 373 K for 10 min in vacuum at $5 \times 10^{-5}$ Torr.

**Table 1** Junction parameters of a few as prepared ($U$) and heat-treated ($T$) Ni/Au-(n)ZnSe Schottky barriers (area = 1 mm$^2$) of different doping concentrations at room temperature

| Barrier metal/ (Junction number) | Doping concentration $N_D$(cm$^{-3}$) | Ideality factor $n$ | | Saturation current density $J_0$(nA · cm$^{-2}$) | | Series Resistance $R_s$(kΩ · cm$^{-2}$) | | Barrier height $\Phi_b$ (eV) | |
|---|---|---|---|---|---|---|---|---|---|
| | | $U$ | $T$ | $U$ | $T$ | $U$ | $T$ | $U$ | $T$ |
| Ni/(N1) | $1.4 \times 10^{14}$ | 7.39 | 6.87 | 12.57 | 11.81 | 180 | 128 | 0.714 | 0.717 |
| Au/(A1) | $1.4 \times 10^{14}$ | 7.2 | 6.48 | 9.84 | 8.92 | 165 | 118 | 0.805 | 0.815 |
| Ni/(N2) | $4.8 \times 10^{14}$ | 5.64 | 5.04 | 17.5 | 16.17 | 72 | 57 | 0.717 | 0.722 |
| Au/(A2) | $4.8 \times 10^{14}$ | 6.03 | 5.36 | 14.6 | 13.4 | 67 | 54 | 0.809 | 0.816 |
| Ni/(N3) | $9.7 \times 10^{14}$ | 4.89 | 4.36 | 25.2 | 21.4 | 15.2 | 8.8 | 0.724 | 0.727 |
| Au/(A3) | $9.7 \times 10^{14}$ | 3.97 | 3.53 | 18.7 | 16.6 | 20.2 | 12.5 | 0.817 | 0.82 |

## 3 Results and Discussion

### 3.1 Current-Voltage Characteristics

Hall-effect and hot-probe measurements confirmed that the films were n-type conductors. The linear $I$–$V$ characteristics at voltages up to 5 V of a sandwich structure of Al-ZnSe with In and Al as the back electrode confirmed that the Al-(n)ZnSe contacts were ohmic. The $I$–$V$ characteristics of both structures of different doping concentrations, as prepared and after the short heat treatment, are shown in Fig. 2. The rectifying nature of $I$–$V$ characteristics of the fabricated structures indicates the existence of Schottky barriers between the thin film of Au and (n)ZnSe and of Ni and (n)ZnSe. The reverse current does not saturate and shows some bias dependence of the barrier height. The current density $J$ of a diode of saturation current density $J_0$ and diode ideality factor $n$, for biasing voltage $V$ and at temperature $T$ are related by [16]

$$J = J_0 \exp(qV/nkT)\left[1 - e^{-qV/kT}\right] \tag{1}$$

The ideality factor and the saturation current density of different junctions as prepared ($U$) and after heat treatment ($T$) were calculated from the slopes and intercepts of the respective $\ln\left[J/(1 - e^{-qV/kT})\right]$ versus $V$ plots (Fig. 3), and are tabulated in Table 1. The diode ideality factor for both structures was found to be much greater than unity and was reduced with heat treatment of the structures. The structures with higher doping concentrations showed an improved diode quality with a reduced diode ideality factor. The presence of an interfacial layer, image-force lowering, and carrier recombination due to surface states or defect levels are some of the main reasons for the ideality factor being greater than unity.

At higher forward voltages, the ln $I$–$V$ plots of the junctions are observed to deviate from linearity. This is due to the series resistance, $R_s$, associated with the neutral region of the semiconductor [17]. At a large forward current through the diode, the voltage drop across the series resistance causes the actual voltage drop across the

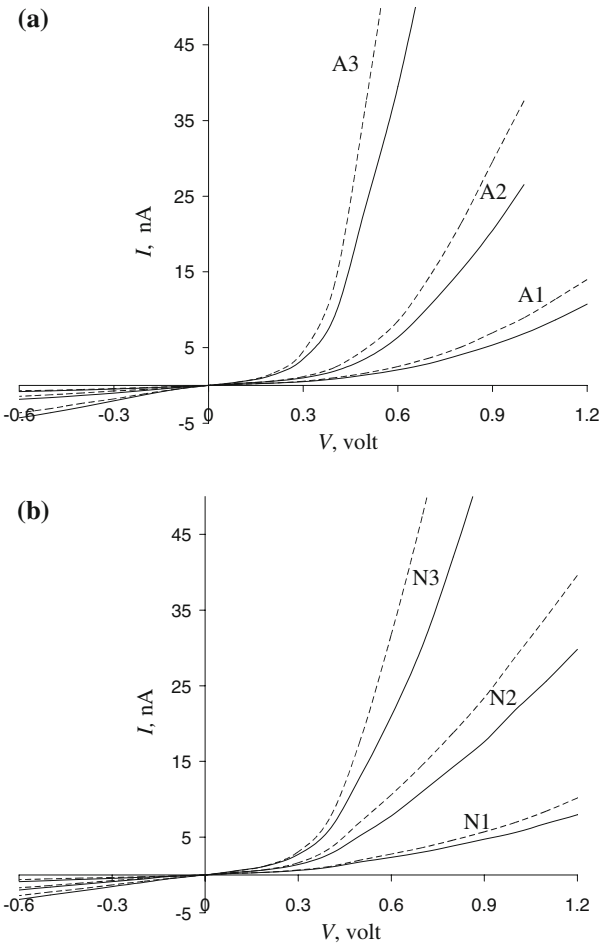


**Fig. 2** *I–V* plots at room temperature in dark of as prepared (*solid line*) and after heat treatment (*dotted line*): (**a**) Au-(n)ZnSe and (**b**) Ni-(n)ZnSe Schottky barrier junctions for different doping concentrations [$1.4 \times 10^{14}$cm$^{-3}$(A1 & N1), $4.8 \times 10^{14}$cm$^{-3}$ (A2 & N2), and $9.7 \times 10^{14}$cm$^{-3}$ (A3 & N3)]

barrier to be less than the voltage applied to the terminals of the structure. Hence, the current is proportional to $[e^{q(V-IR_s)/kT} - 1]$, instead of obeying the ideal condition. The horizontal displacement between the actual ln *I–V* curve and extrapolation of the linear region gives the voltage drop $\Delta V = I R_s$ across the neutral region.

The series resistance of the Au/Ni-(n)ZnSe junctions, calculated from the *I* versus $\Delta V$ plots (not shown here), are given in Table 1 and are on the order of kΩ. The large value is due to various types of defects that crept into the film during preparation, and also due to the low doping concentration. The series resistance of the junctions of higher doping concentration was found to be less. The introduction of any insulating layer between the electrode and semiconductor also contributes to the series resistance. With the present method of preparation of the devices, some interfacial layer is developed due to breaking of vacuum between the deposition of each layer. Heat

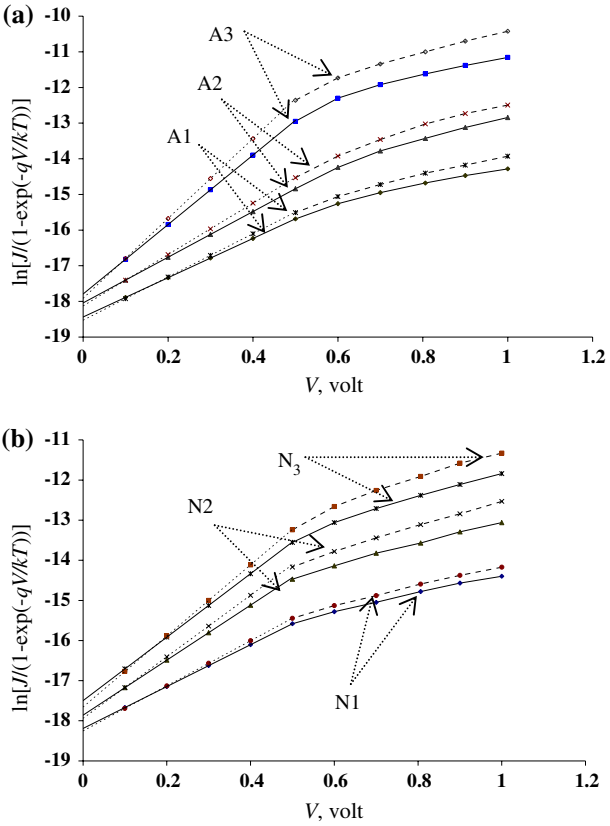


**Fig. 3** $\ln[J/(1-\mathrm{e}^{-qV/kT})]$ versus $V$ plots at room temperature in dark of as prepared (*solid curve*) and heat treated (*dotted curve*): (**a**) Au-(n)ZnSe and (**b**) Ni-(n)ZnSe Schottky barrier junctions for different doping concentrations [$1.4 \times 10^{14}\mathrm{cm}^{-3}$(A1 & N1), $4.8 \times 10^{14}\mathrm{cm}^{-3}$ (A2 & N2), and $9.7 \times 10^{14}\mathrm{cm}^{-3}$ (A3 & N3)]

treatment of the devices reduces the defects in the film and ensures more intimate contact between the electrodes and semiconductor by thermally removing the insulating layer. Therefore, the series resistance of the devices is found to be reduced with heat treatment.

The temperature dependence of $J$–$V$ characteristics of the junction has been studied within the temperature range from 300 K to 333 K. It has been observed that beyond room temperature, thermal generation of extra carriers causes a gradual increase of the forward current. Figure 4 shows $\ln[J/(1-\mathrm{e}^{-qV/kT})]$ versus $V$ plots of the linear portion for a typical Au-(n)ZnSe junction at different temperatures from which the $J_0$ values at different temperatures were calculated. At all temperatures, the ideality factor was found to be nearly the same value and the saturation current density is found to increase with temperature. When $\ln(J_0/T^2)$ versus $T^{-1}$ is plotted (Fig. 5), a straight line is found indicating that the transport process is dominated by thermionic emission, according to [18]

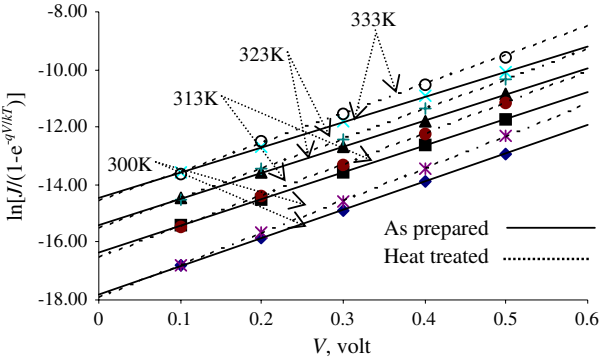


**Fig. 4** $\ln[J/(1-e^{-qV/kT})]$ versus $V$ plots of a typical Au-(n)ZnSe junction (A3) ($N_D = 9.7\times10^{14}$ cm$^{-3}$) at different temperatures

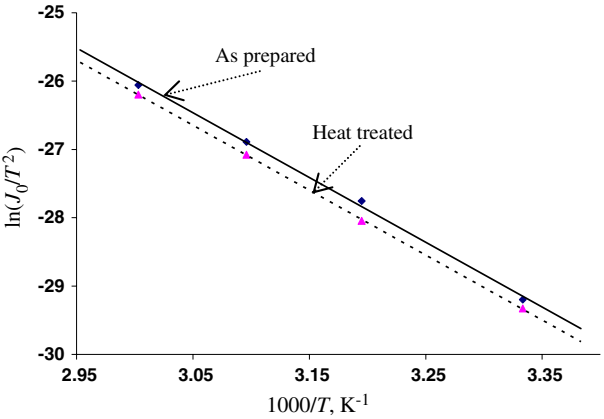


**Fig. 5** $\ln(J_0/T^2)$ versus $T^{-1}$ plots of a typical Au-(n)ZnSe junction (A3) ($N_D = 9.7\times10^{14}$ cm$^{-3}$)

$$J_0 = A^*T^2e^{-q\Phi_b/kT}, \tag{2}$$

where $\Phi_b$ is the barrier height of the junction and $A^*$ is the effective Richardson constant.

The value of $A^*$ was calculated from the intercept on the vertical axis of the plots, and the barrier height of the junction was estimated from its slope. The barrier heights were found to be in the range of 0.71 eV to 0.82 eV (Table 1). This is in good agreement with the values reported earlier [19]. However, higher barrier heights of 1.65 eV and 1.2 eV for single crystal ZnSe with Au and Ni, respectively, have been reported by other workers [20,21]. From the table it is seen that there are no significant changes of barrier height with doping concentrations, and the heat treatment applications result in slight increases of the barrier heights. The lower value of the barrier height is due to the presence of the interfacial layer. In polycrystalline semiconductor thin films, the constituent atoms at the grain boundary are disordered, and hence, there are large numbers of defects due to incomplete atomic bonding (dangling bond). This may result

**Table 2** Photovoltaic parameters of as prepared (*U*) and heat-treated (*T*) Au/Ni-(n)ZnSe Schottky barrier junctions of 1 $mm^2$ area for different doping concentrations at room temperature

| Barrier metal | Junction number | Doping concentration $N_D$ ($cm^{-3}$) | Short-circuit current density $J_{sc}$ ($\mu A \cdot cm^{-2}$) | | Open-circuit voltage $V_{oc}$ (mV) | | Fill factor | |
|---|---|---|---|---|---|---|---|---|
| | | | *U* | *T* | *U* | *T* | *U* | *T* |
| Ni | N1 | $1.4 \times 10^{14}$ | 0.173 | 0.215 | 550 | 490 | 0.30 | 0.33 |
| Au | A1 | $1.4 \times 10^{14}$ | 0.10 | 0.123 | 365 | 385 | 0.31 | 0.32 |
| Ni | N2 | $4.8 \times 10^{14}$ | 0.28 | 0.331 | 400 | 420 | 0.34 | 0.37 |
| Au | A2 | $4.8 \times 10^{14}$ | 0.278 | 0.326 | 365 | 390 | 0.34 | 0.36 |
| Ni | N3 | $9.7 \times 10^{14}$ | 0.390 | 0.440 | 420 | 370 | 0.40 | 0.43 |
| Au | A3 | $9.7 \times 10^{14}$ | 0.412 | 0.46 | 300 | 280 | 0.39 | 0.42 |

in the existence of surface states [22]. In our case, the barrier heights have been found to be less dependent on the work function of the barrier metals. These may be due to the effect of surface states of the semiconductor [23]. Similar behavior was observed in Schottky barriers of other II–VI semiconductors including ZnSe [24].

### 3.2 Photovoltaic Effect

The Au/Ni-(n)ZnSe junctions were studied under illumination for their photovoltaic performance. Figure 6 shows the photovoltaic response of a few typical junctions of different doping concentrations at room temperature under illumination of intensity 0.5 $mW \cdot mm^{-2}$. At lower doping concentrations, the nearly linear nature of the *J*–*V* curve under illumination implies the existence of a very high series resistance in the junctions. The open-circuit voltage ($V_{oc}$), short-circuit current ($I_{sc}$), and fill factor of these junctions are tabulated in Table 2. The short-circuit currents were found to be 0.173 $\mu A \cdot cm^{-2}$ to 0.412 $\mu A \cdot cm^{-2}$ for junctions of doping concentrations of $1.4 \times 10^{14}$ $cm^{-3}$ to $9.7 \times 10^{14}$ $cm^{-3}$, respectively. The fill factor of the junctions was increased from 0.31 to 0.40 with an increase of the doping concentration from $1.4 \times 10^{14}$ $cm^{-3}$ to $9.7 \times 10^{14}$ $cm^{-3}$ and was further increased up to 0.43 after heat treatment.

The open-circuit voltage and short-circuit current are strongly dependent on the series resistance as well as on the diode ideality factor as per the well-known equations [25],

$$I_{sc} = I_0 \left[\exp\{q\,(V - I R_S)\,/kT\} - 1\right] - I \tag{3}$$

$$V_{oc} = (nkT/q) \ln\left[(I_{sc}/I_0) + 1\right] \tag{4}$$

where $I$ is the total output current and $I_0$ is the diode saturation current. In our case, the higher value of the series resistance reduces the short-circuit current and, hence, also the open-circuit voltage. Very low photo-voltages with low fill factors have been

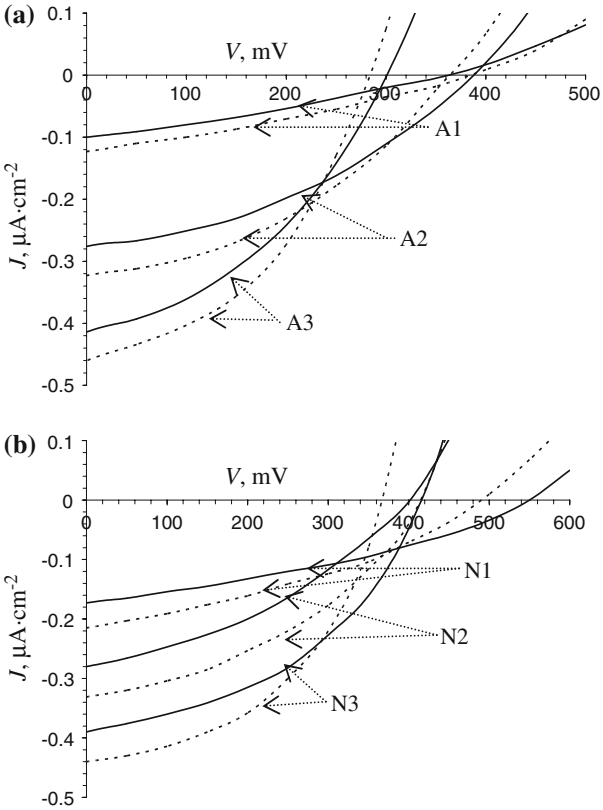


**Fig. 6** Photovoltaic plots of as prepared (*solid curve*) and heat treated (*dotted curve*) (**a**) Au-(n)ZnSe and (**b**) Ni-(n)ZnSe Schottky barrier junctions of different doping concentrations [$1.4 \times 10^{14}$ cm$^{-3}$(A1 & N1), $4.8 \times 10^{14}$ cm$^{-3}$ (A2 & N2), and $9.7 \times 10^{14}$ cm$^{-3}$ (A3 & N3)] at room temperature

observed in these junctions due to the higher value of diode ideality factors. In the polycrystalline films, the grain-boundary potential may affect the series resistance and open-circuit voltage of solar cells [26]. Due to this grain-boundary effect, recombination of photo-generated carriers takes place at grain boundaries, and hence, the short-circuit current is reduced [26,27]. Besides the effect of the high series resistance and grain-boundary effects, other factors may be responsible for the poor photovoltaic performance, including a high defect density, the presence of interfacial layer, and low doping concentration. The increase of the doping concentration of the semiconducting films and heat treatment slightly improves the photovoltaic performance of the devices.

## 4 Conclusions

The results show the formation of Schottky barriers in thermally deposited Au-(n)ZnSe and Ni-(n)ZnSe thin-film structures with a thin interfacial layer and are characterized

by non-saturating and bias-dependent reverse currents and higher values of diode ideality factors. The junctions exhibited rectifying characteristics and a low photovoltaic effect. Due to various types of defects and low doping concentrations, the junctions have high series resistances. The presence of an interfacial layer, surface states, and various defects are found to affect the *I–V* characteristics and photovoltaic effect. The performance of the diodes was improved after short heat treatment. This improvement is thought to be due to reduction of the interfacial layer and interface state densities. Proper doping, annealing, and passivation of surface states are necessary to improve the diode quality and photovoltaic effect. The deposition of all the layers in one vacuum cycle might be advantageous.

**Acknowledgments** Two of the authors (Sumbit Chaliha and Mothura Nath Borah) wish to thank the University Grant Commission of India, for awarding teachers fellowship to carry out this research works.

## References

1. A.P. Samantilleke, I.M. Darmadasa, K.A. Prior, K.L. Choy, J. Mei, R. Bacewicz, A. Wolska, J. Mater. Sci.-Mater. Electron. **12**, 661 (2001)
2. E. Kato, H. Noguchi, M. Nagai, H. Okuyama, S. Kijima, A. Ishibashi, Electron. Lett. **34**, 282 (1998)
3. F. Vigue, E.Tournib, J.P. Faurie, Electron. Lett. **36**, 352 (2000)
4. J.-B. Yoo, A.L. Fahrenbruch, R.H. Bube, Solar Cells **31**, 171 (1991)
5. T.L. Chu, S.S. Chu, G. Chen, J. Britt, C. Ferekides, C.Q. Wu, J. Appl. Phys. **71**, 3865 (1992)
6. R.B. Kale, C.D. Lokhande, Appl. Surf. Sci. **252**, 929 (2005)
7. M.E. Sherif, F.S. Terra, S.A. Khodier, J. Mater. Sci.-Mater. Electron. **7**, 391(1996)
8. S. Venkatachalam, D. Mangalaraj, S.K. Narayandass, S. Velumani, P. Schabes-Retchkiman, J.A. Ascencio, Mater. Chem. Phys. **103**, 305 (2007)
9. P. Besomi, B.W. Wessels, Electron. Lett. **16**, 794 (1980)
10. M. Vos, F. Xu, J.H. Weaver, Appl. Phys. Lett. **53**, 1530 (1988)
11. W.D. Gill, R.H. Bube, J. Appl. Phys. **41**, 3731 (1970)
12. S. Tolansky, *Multiple Beam Interferomerty of Surfaces and Films* (Oxford University Press, London, 1948)
13. M.N. Borah, S. Chaliha, P.C. Sarmah, A. Rahman, Indian J. Pure Appl. Phys. **45**, 687 (2007)
14. W.R. Runyem, *Semiconductor Measurements and Instrumentation* (McGraw-Hill, New York, 1975), p. 144
15. P.C. Sarmah, A.Rahman, Bull. Mater. Sci. **21**, 149 (1998)
16. E.H. Rhoderik, *Metal Semiconductor Contacts* (Clarendon Press, Oxford, 1978), p. 87
17. E.H. Rhoderik, *Metal Semiconductor Contacts* (Clarendon Press, Oxford, 1978), p. 7
18. S.M. Sze, *Physics of Semiconductor Devices*, 2nd edn. (Willey Eastern Ltd., New Delhi, 1986), p. 259
19. R. Coratger, C. Girardin, J. Beauvillain, I.M. Dharmadasa, A.P. Samanthilake, J.E.F. Frost, K.A. Prior, B.C. Cavenett, J. Appl. Phys. **81**, 7870 (1997)
20. L. Tarricone, Rev. Phys. Appl. **15**, 1617 (1980)
21. V.P. Makhnii, Tech. Phys. **43**, 1119 (1998)
22. J.M. Pawlikoski, Thin Solid Films **190**, 39 (1990)
23. J. Bardeen, Phys. Rev. **71**, 717 (1947)
24. I.M. Dharmadasa, Prog. Cryst. Growth Charact. **36**, 249 (1998)
25. G. Wary, T. Kachary, A. Rahman, Int. J. Thermophys. **27**, 332 (2006)
26. T.L. Chu, S.S. Chu, Solid State Electron. **38**, 533 (1995)
27. J. Dutta, D. Bhattacharyya, S. Chaudhuri, A.K. Pal, Sol. Energy Mater. Sol. Cells **36**, 357 (1995)